CrossMark

Polyatomic interferences on high precision uranium isotope ratio measurements by MC-ICP-MS: applications to environmental sampling for nuclear safeguards

Anthony D. Pollington[1] · William S. Kinman[1] · Susan K. Hanson[1] · Robert E. Steiner[1]

Abstract Modern mass spectrometry and separation techniques have made measurement of major uranium isotope ratios a routine task; however accurate and precise measurement of the minor uranium isotopes remains a challenge as sample size decreases. One particular challenge is the presence of isobaric interferences and their impact on the accuracy of minor isotope ^{234}U and ^{236}U measurements. We present techniques used for routine U isotopic analysis of environmental nuclear safeguards samples and evaluate polyatomic interferences that negatively impact accuracy as well as methods to mitigate their impacts.

Keywords Multi collector inductively coupled plasma mass spectrometry (MC-ICP-MS) · Environmental sampling for nuclear safeguards · Uranium isotopes · Polyatomic interferences

Introduction

Over the last two decades, environmental sampling for nuclear safeguards has significantly expanded as a result of numerous advances in detection technology (e.g., [1–4]). Measurement of uranium (U) and plutonium (Pu)

✉ Anthony D. Pollington
pollington@lanl.gov

[1] Nuclear and Radiochemistry, Los Alamos National Laboratory, MS J514, P.O. Box 1663, Los Alamos, NM 87545, USA

abundances and their isotopic compositions are particularly challenging in environmental samples due to generally low analyte concentrations. Accurate and precise measurements of the minor isotopes ^{234}U and ^{236}U are increasingly difficult as the overall U concentration available for analysis decreases. The abundance of ^{236}U in natural U is exceptionally low ($^{236}U/^{238}U \sim 1$–50×10^{-10}; [5–8]), and the presence of significant ^{236}U in a sample provides evidence that a U material has experienced a neutron flux [9]. An ongoing goal in environmental safeguards sample analysis is to provide the maximum amount of useful compositional data from a minimum amount of sample. In this study we describe an enhanced sample introduction system interfaced with a multicollector inductively coupled plasma mass spectrometer (MC-ICP-MS) used for routine environmental-level U isotopic analysis of environmental nuclear safeguards samples. The MC-ICP-MS is equipped with multiple electron multiplier ion counters for improved accuracy and precision of low-level U isotopic analysis. While the enhanced analytical setup results in a tenfold sensitivity enhancement at ^{238}U, as sample size decreases the potential negative impacts of polyatomic interferences (PAI) increase. We present and discuss PAI observed during analysis of environmental safeguards samples that interfere with uranium isotopes and present radiochemical purification and analysis strategies to mitigate them.

Analytical challenges highlighted by real samples

Over the course of 24 months in our capacity as a network analytical laboratory (NWAL) for environmental sample analysis for the International Atomic Energy Agency (IAEA), all samples received for analysis were screened following thermal ashing and subsequent dissolution to identify the presence of elements that might negatively

Springer

impact efforts to produce highly purified U and Pu fractions for analysis. Aliquots consisting of 1 % of each primary dissolution solution were taken by mass and diluted to a total volume of 5 mL in 0.32 M HNO_3 for multielement analysis using a single collector ICP-MS (Thermo Element XR). The screening routine was largely qualitative for elements other than U and includes measurement of ~86 isotopes between masses 6 and 249. We have regularly observed samples with exceptionally high count rates at masses corresponding to [204]Pb, [206]Pb, [207]Pb, and [208]Pb. We have also observed select samples with exceptionally high count rates at masses corresponding to isotopes of Pt, Fe, Cr, and W, among other elements. Platinum and Pb-based polyatomic interferences are particularly worrisome, as various combinations of Pt or Pb isotopes with O, N, or Ar interfere with isotopes of U (Table 1).

Experimental

Interferences affecting uranium

Polyatomic ions form in the plasma and interface regions of an ICP-MS and must be considered if their nominal masses interfere with isotopes of interest (e.g., [10–14]). Mitroshkov et al. [14] suggested that polyatomic species interfering with isotopes of Pu were significantly reduced by using a desolvating nebulizer. Oh et al. [13] presented formation rates for PAI formed from pure standard solutions using a desolvating nebulizer, but did not discuss the differences between sample introduction systems, nor provide examples from real samples or recommendations for mitigating PAI formation. The effectiveness of desolvation on reducing polyatomic interferences that impact uranium analyses has not been thoroughly investigated, and a key objective of this study was to evaluate the formation and mitigation of PAI that have been observed in actual environmental safeguards samples. Platinum argide (PtAr) PAI have the potential to significantly interfere with isotope masses of U (Table 1). The major isotopes of Pt (194,

195, 196, and 198) can each combine with [40]Ar to create interferences with [234]U, [235]U, [236]U and [238]U (Table 1). These PAI have masses slightly different from the mass of the corresponding U isotope, and could theoretically be separated by using medium or high resolution ICP-MS. However, losses in ion transmission (nominally a 90 % reduction for MR and 97 % for HR) are too great when sample size is limited. Significant interferences from the combination of the stable Pb isotopes (204, 206, 207, 208) with low mass elements that are present in the atmosphere and sample solution (e.g., H, C, N, O) can also negatively affect the accuracy of U isotopes measured.

In this study, we consider only the major isotopes of elements known to combine with gaseous impurities to form PAI (^{14}N, ^{16}O, [40]Ar), although combinations including minor isotopes of all of these elements may also yield non-trivial impacts on major and minor U isotopes. Additionally, PAI considered are limited to a maximum of three atoms (e.g., [208]Pb[14]N[14]N$^+$ interfering on [234]U$^+$ was considered, but [208]Pb[14]N[14]N[1]H$^+$ interfering on [235]U$^+$ was not considered). Table 1 lists the isotopes of U, and the most likely interfering species from Pt and Pb PAI combinations. See also Mitroshkov et al. [14] for a discussion of PAI that affect Pu measurements.

Samples

To investigate the formation rates of Pt- and Pb-based PAI, and the effect of the desolvating nebulizer on formation rates, solutions containing varying concentrations of Pt and Pb were prepared for analysis. Platinum solutions were diluted to 100 and 10 ppb from a 1000 ppm single element Pt standard (RICCA chemical catalog # PPT1KH-100). Lead solutions were diluted to 200, 30 and 20 ppb (NBS-981, -982), and 100, 15 and 10 ppb (NBS-983). Samples were prepared by diluting solutions of known concentration with high purity 0.32 M HNO_3. Archived fractions of dissolved environmental safeguards samples identified as having elevated concentrations of Pt, Pb or other elements with the potential to form interfering PAI were used to test

Table 1 Possible interferences from Pb and Pt in the U mass range

Uranium isotope of interest	Possible argide interference, MRP needed[a]	Possible oxide interference, MRP needed[a]	Possible nitride interference, MRP needed[a]	Possible nitrogen–oxygen interference, MRP needed[a]
[234]U	[194]Pt[40]Ar (2020)		[206]Pb[14]N[14]N (3879)	[204]Pb[14]N[16]O (3347)
[235]U	[195]Pt[40]Ar (2013)		[207]Pb[14]N[14]N (3798)	
[236]U	[196]Pt[40]Ar (1997)	[204]Pb[16]O[16]O (2855)	[208]Pb[14]N[14]N (3761)	[206]Pb[14]N[16]O (3229)
[238]U	[198]Pt[40]Ar (1976)	[206]Pb[16]O[16]O (2752)		[208]Pb[14]N[16]O (3126)

[a] MRP needed, which is shown in parentheses, is the mass resolving power needed to separate the isotope of interest from the interference with nominally the same mass. $MRP = m/\Delta m$ where m is the mass of the isotope of interest and Δm is the difference between the mass of the isotope and the mass of the interference

various radiochemical U purification approaches. Environmental safeguards samples consist of 10 cm × 10 cm cotton swipes collected at nuclear sites by IAEA inspectors [1] and contain highly variable matrices that are dependent on the types of materials and surfaces swiped.

Instrumentation

Uranium isotope ratio measurements were made using a Thermo Neptune Plus ICP-MS. The Neptune Plus is equipped with a double-focusing Nier-Johnson geometry sector-field mass analyzer, and is equipped with ten Faraday cups (FC) (eight movable, two fixed position) and six ion-counting (IC) detectors (one movable, five fixed position) (Table 2; Supplemental Fig. 1). The axial position consists of a fixed position Faraday cup and a full-size secondary electron multiplier (SEM) IC; the beam is focused into the FC or IC by means of deflection plates. The axial IC sits behind a retarding potential quadrupole (RPQ) that can be used to improve abundance sensitivity by acting as a secondary electrostatic filter. The "Plus" module consists of an array of fixed position FC and IC's on the low mass side of the L4 cup. A set of beam guides steers ions to the axial IC, two additional full size SEMs (one with a selectable RPQ), a selectable FC and two fixed position compact discrete dynode (CDD) ICs at the lowest mass positions.

There is a moveable CDD attached to the low mass side of the L3 FC (Table 2; Supplemental Fig. 1). This particular package is custom designed for the simultaneous analysis of low concentration U isotopes: ^{238}U can be analyzed on either a FC (L4) or movable IC (CDD attached to L3), ^{236}U on a full size SEM with optional RPQ, ^{235}U either on a FC or full size SEM, ^{234}U on a full size SEM with optional RPQ and ^{233}U on a CDD. The RPQ's on ^{236}U and ^{234}U can be activated to decrease contributions from the signal tails of ^{238}U and ^{235}U. Faraday detectors were cross-calibrated before each analytical session using an internally supplied voltage that is stepped across each FC to measure and record the response of each detector. Faraday detector gain calibrations were updated using a manufacturer supplied gain calibration routine. Ion counters were cross calibrated using a U solution with ^{238}U

concentration sufficient to be measured both on either a FC or an IC (0.005 V signal on an FC or 312,500 cps on an IC). The ratio of the signal measured on the IC to the signal measured on the FC was used to determine individual IC yields. Yields for full size SEM ICs were adjusted to ≥93 %, and CCD ICs were set between 99.5 and 100.5 % by adjusting the IC operating voltage. Ion counter yields were determined before each analytical session and were monitored within analysis sessions via inclusion of cross calibration samples within analysis sequences.

For measurements utilizing a 'standard' sample introduction system, a cyclonic glass spray chamber equipped with an Elemental Scientific PFA-ST nebulizer coupled to a 0.50 mm ID uptake tube was interfaced with the MC-ICP-MS with standard sample and skimmer (H) cones. With this setup, a typical sensitivity is ∼100 V/ppm for ^{238}U. To increase sensitivity, a CETAC Aridus II was interfaced with the MC-ICP-MS equipped with either standard cones or a Jet-type sample cone and an X-type skimmer cone. The X skimmer cone has a different taper angle than the standard H cone. The Aridus II system uses Ar and N_2 sweep gases, a desolvating membrane, a heated spray chamber and a low-flow PFA nebulizer to generate a dry aerosol. The low-flow nebulizers used for this experiment have nominal uptake rates of 100 μL/min and measured uptakes of ∼70 μL/min, as compared to ∼400 μL/min for the nebulizers used with the standard glass spray chamber. To test formation of polyatomic species under different conditions, three sample introduction combinations were used in this study: (1) cyclonic glass spray chamber with standard sample and skimmer cones, (2) Aridus II with standard sample and skimmer cones, (3) Aridus II with enhanced sample (jet) and skimmer (X) cones (Table 3).

Results and discussion

We observed significant formation of the PtAr$^+$ PAI when using both a standard glass spray chamber ("wet plasma") and the Aridus II desolvating nebulizer ("dry plasma").

Table 2 Detector setup on Thermo Neptune Plus showing optional methods for simultaneous collection of U isotopes

Detector Name	H4	H3	H2	H1	C/IC1C	L1	L2	L3	IC6	L4	IC1B	L5/IC2	IC3	IC5	IC4
Detector type	FC	FC	FC	FC	FC/SEM	FC	FC	FC	CDD	FC	SEM	FC/SEM	SEM	CDD	CDD
Method1										^{238}U	^{236}U	^{235}U	^{234}U	^{233}U	
Method2									^{238}U		^{236}U	^{235}U	^{234}U	^{233}U	

Faraday cups H1–H4 and L1–L4 are movable. IC6 is attached to L3 and is therefore movable, all other detectors are in fixed positions

*FC* Faraday cup, *SEM* full size secondary electron multiplier, *CDD* compact discrete dynode

Table 3 Argide and oxide formation rates with and without Aridus II

Spray chamber	Cones	Pb standard	Pt (ppb)	Pb (ppb)	Pt sensitivity (V/ppb)	Pb sensitivity (V/ppb)	$^{196}Pt^{40}Ar/^{196}Pt$	$^{206}Pb^{16}O/^{206}Pb$	$^{206}Pb^{40}Ar/^{206}Pb$
Glass	Standard	NBS 981	100	200	0.0666	0.0845	3.99E−5	1.04E−5	2.21E−6
Aridus II	Standard	NBS 981	10	30	0.0952	0.2262	1.50E−4	2.24E−7	1.59E−6
Aridus II	Jet/X	NBS 981	10	20	0.2650	0.7383	3.64E−4	5.94E−7	4.24E−5

Figure 1 compares the shapes and relative positions of peaks observed by scanning the instrument's magnet across masses 234, 235, 236 and 238 while aspirating solutions of Pt-free uranium (40 ppt NBL CRM U-010) or U-free Pt (100 ppb Pt solution). Overall, for a given Pt concentration, greater contributions from the $PtAr^+$ PAI were observed at nominal U masses of interest using a desolvating nebulizer than with a standard spray chamber (Table 3).

We observed formation of both the $PbAr^+$ and PbO^+ PAI in Pb solutions measured using a standard glass spray chamber and using an Aridus II desolvating nebulizer (Fig. 2; Table 3). It is clear from Fig. 2a, b that while significant lead oxide and lead hydroxide molecules are formed in a wet plasma using a standard spray chamber, PAI comprised of Pb plus one N, two O or two N atoms do not significantly impact the observed signals for uranium isotopes of interest. The origin of the peaks observed in the mass range 227-231 for the standard spray chamber is not readily apparent, although the shape of the spectrum suggests that this is caused by the combination of Pb with something of mass 23 (Fig. 2a). Whether this is Na or some other compound (e.g., $^4He^{19}F$) is not clear. However, this species does not affect the measurement of U isotopes and its identity is not considered further in this study. There are signals at masses 234 and 236 in the Aridus II generated spectrum that may be attributed to $Pb^{14}N_2$ molecules. The Aridus II makes use of N_2 additional gas, which may explain an increase of N_2 based molecules when using this sample introduction system. The pattern does not exactly match with the expected spectrum from Pb (i.e., measured 234 and 236 counts are equal, whereas if these were $^{206}PbN_2$ and $^{208}PbN_2$, the counts at 236 should be $\sim 2\times$ those at 234), and further investigation is required. In general, we observed that the use of the Aridus II desolvating nebulizer greatly reduced the formation of oxide-based PAI but led to greater formation of argide-based PAI.
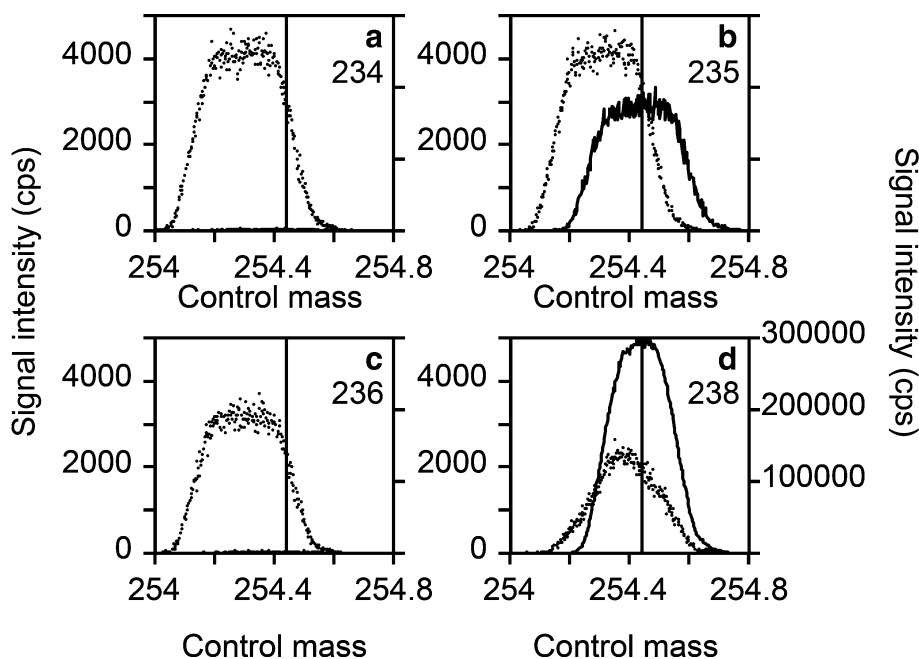
Fig. 1 Peak scans over U mass range in Pt and U standards using a glass spray chamber. Each *panel* represents signals measured for a given mass/charge ratio collected on a single detector in a fixed position; e.g., in *panel b* ^{235}U and $^{195}Pt^{40}Ar$ are collected on IC2 (Supplemental Fig. 1). *Solid traces* represent U isotopes, *dotted traces* represent PtAr ions; *vertical line* represents the mass setting for U isotopes. The offset of the *dotted traces* indicate that these are not U isotopes. The signals for most of the PtAr ions are much larger than the signals for the given U isotopes. The *vertical scales* of each figure are the same, except for the ^{238}U counts, which are indicated on the *right vertical axis* of *panel d*. See also Supplemental Fig. 2
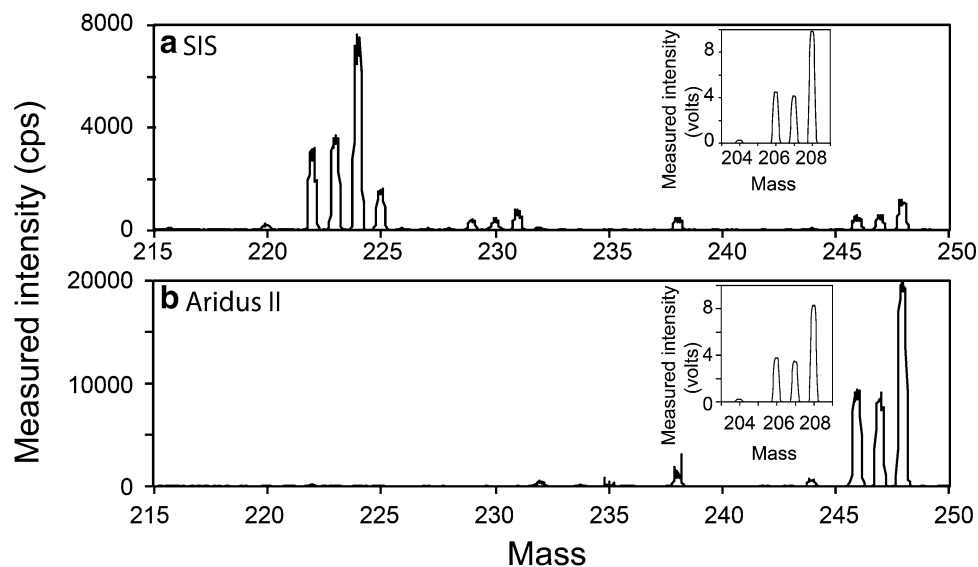
Fig. 2 Mass scans of NBS-981 Pb solution using the standard setup and Aridus II. *Insets* show signals caused by Pb; this pattern can be compared to higher masses to determine if signals are caused by combinations of Pb with other elements. *a* Mass scan of 200 ppb NBS-981 solution using SIS. Masses from 220 to 225 are caused by PbO and PbOH ions. *b* Mass scans of 20 ppb NBS-981 solution using the Aridus II with jet and X-cones. Note that while PbAr ions are still present, PbO and PbOH ions are significantly reduced. Signals at 232, 235 and 238 are from contamination from Th and U
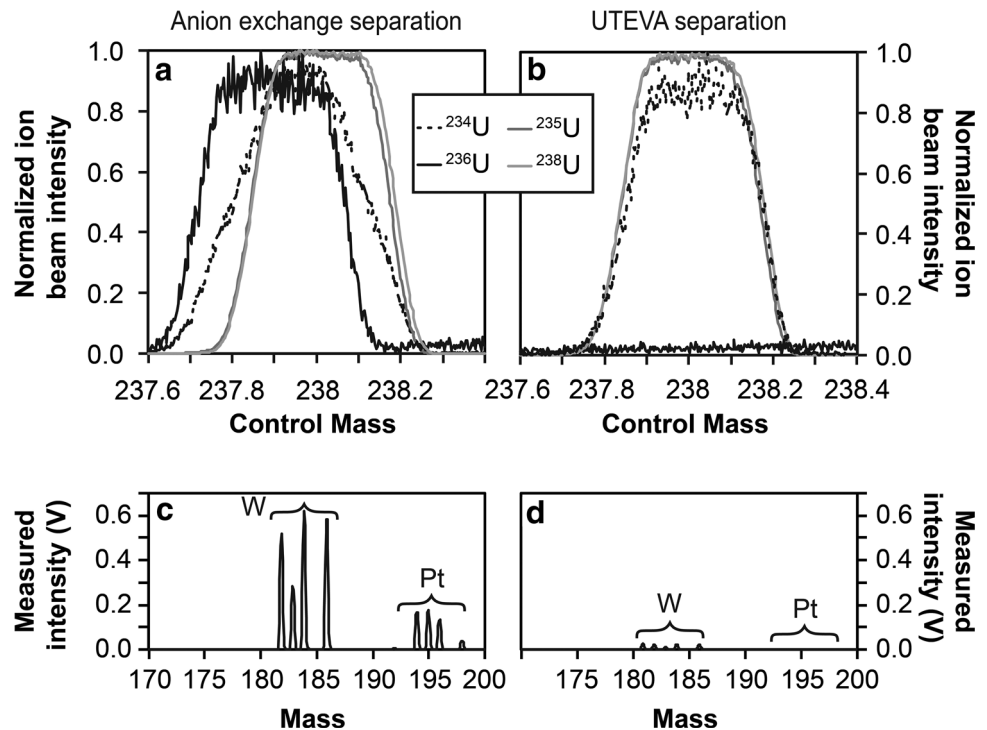
Observations in this study are consistent with the conclusions of Mitroshkov et al. [14] that oxide and hydride formation is reduced by use of a desolvating nebulizer but contradict the conclusion that argide formation is also decreased. Mitroshkov et al. [14] particularly note that PAIs from Hg are reduced compared to previous studies (the major isotopes of Hg all have argide interferences at isotope masses of Pu, the element of interest in their study). It is clear from our observations that U chemical purification efforts prior to analysis must adequately remove Pt and Pb to improve the likelihood of making an accurate U isotope ratio measurement.

Effective removal of platinum and lead from U fractions

While Pb is a more common contaminant in environmental safeguards samples given the large amount of Pb used for shielding in nuclear facilities, the investigation of Pt as a potential interference is not just an academic exercise. A recent routine environmental safeguards sample processed by our laboratory was observed to contain a significant amount of Pt during routine screening ($\sim$50 ng total Pt in the sample). An initial U purification was performed using an anion exchange method to purify the U fraction. The anion exchange method is described briefly: the U aliquot was selected based upon aforementioned screening results and was evaporated to dryness, treated with 1 mL concentrated HCl, evaporated to dryness, dissolved in a HCl-Cl$_2$ solution

(10 mL concentrated HCl + 2 drops 30 % H$_2$O$_2$) and loaded onto a 1 mL column of AG MP-1 (100–200 mesh) anion exchange resin. The resin bed was washed with HCl-Cl$_2$ followed by washes with an HCl-HI solution (9 mL concentrated HCl + 1 mL concentrated HI), then U was eluted with 8 M HNO$_3$. A qualitative mass scan of the U fraction using anion exchange clearly shows peaks at masses 234 and 236 with non-flat-top shape and peak centroids that are shifted from the accurate U masses (Fig. 3a), which indicates that despite efforts to purify U, an element contributing to the formation of a PAI is present. A qualitative mass scan from mass 170–200 revealed relatively high concentrations of W and Pt in the purified U fraction and that the likely PAIs are ^{194}Pb^{40}Ar$^+$ and ^{196}Pb^{40}Ar$^+$ (Fig. 3c). Subsequent to this discovery, the aliquot was subjected to an additional U purification using UTEVA resin from Eichrom Technologies, LLC., then reanalyzed. The UTEVA U purification method is summarized briefly: the U aliquot was evaporated to dryness then dissolved in 3 M HNO$_3$. A column of 2 ml UTEVA resin (100–150 μm) was prepared, washed with 18.2 MΩ H$_2$O and conditioned with 3 M HNO$_3$; the sample was loaded and the column was washed with 3 M HNO$_3$, 9 M HCl, then 5 M HCl–0.05 M oxalic acid. Finally U was eluted with 1 M HCl. Typical blanks using the UTEVA method have been $\sim$10 pg ^{238}U over the past 6 months compared to typical U analysis fractions consisting of 2–3500 ng total U. Figure 3b, d shows that the vast majority of Pt and W in the sample was removed using a UTEVA-based U purification. The improved chemical purification

was particularly evident when examining the shape and position of the 236 peak: following U purification using only the anion exchange method, a clear signal was measured above instrumental background at mass 236 (Fig. 3a). Following purification using UTEVA chemistry, the intensity measured at 236 is fully attributable to tailing from ^{238}U. The absence of the signal at 236 in the highly purified sample confirms that the observed signal arose from a polyatomic interference and *there is no ^{236}U in this sample* (Fig. 3b). The elimination of polyatomic interferences of this type is crucial to ensure the accurate detection of ^{236}U in environmental safeguards samples. Reporting positive detections of ^{236}U should thus be accompanied by a careful evaluation of U purification chemistry and an assessment of what other elements are present in the sample that might combine with elements such as O and Ar to interfere at mass 236.

Conclusions/recommendations

The presence of Pt in a sample, even at low concentrations, can adversely affect the accuracy of U isotope ratios measured by ICP-MS. The use of a desolvating nebulizer, while effective at improving sensitivity and removing oxide, hydride, and hydroxide polyatomic interferences, leads to *greater* formation of argide interferences that may impact major and minor U isotope measurements. Effective

purification is critical to ensure the highest degree of accuracy and precision when measuring U isotope ratios by ICP-MS. The anion exchange chemical purification method previously employed by our laboratory for routine U analysis in environmental safeguards samples did not sufficiently remove Pt from purified U fractions, which lead to a false positive detection of ^{236}U in an environmental safeguards sample. Uranium purifications performed using Eichrom UTEVA resin more effectivley removed Pt, which helped mitigate the formation of problematic PAI.

The discovery of interfering species in a sample presumed to be pure U is possible only by carefully screening each solution prior to analysis and understanding the limitations of various chemical purification schemes. At a minimum, it is prudent to perform qualitative mass scans across peak positions in the U mass range prior to analysis. If distorted or offset peaks are observed (e.g., Fig. 3a), an alternative purification strategy should be considered. Observations associated with real-world enviornmental nuclear safeguards samples prompted our adoption of a UTEVA extraction chromatography U purification method for routine use in our role as an NWAL laboratory for environmental sample analysis for the IAEA. The negative impacts of a false positive detection of ^{236}U, or incorrect U isotopic composition, far outweigh the benefits of the speed allowed by not screening each sample and adherence to U separation methodology historically used by environmental analysis laboratories.

References

1. Donohue DL (1998) Strengthening IAEA safeguards through environmental sampling and analysis. J Alloy Compd 271:11–18
2. Donohue DL (2002) Key tools for nuclear inspections: advances in environmental sampling strengthen safeguards. IAEA Bull. 44(2):17–23
3. Mayer K, Wallenius M, Fanghanel T (2007) Nuclear forensic science—from cradle to maturity. J Alloy Compd 444:50–56
4. Bouman, C, Lloyd, NS, Schwieters JB (2011) Advances in multicollector ICPMS for precise and accurate isotope ratio measurements of Uranium isotopes. Abstract V33G-01 presented at 2011 Fall Meeting, AGU. San Francisco, Calif., 5–9 Dec
5. Zhao XL, Nadeau MJ, Kilius LR, Litherland AE (1994) The 1st detection of naturally-occurring ^{236}U with accelerator mass-spectrometry. Nucl Instrum Methods B 92(1–4):249–253
6. Zhao XL, Kilius LR, Litherland AE, Beasley T (1997) AMS measurement of environmental ^{236}U preliminary results and perspectives. Nucl Instrum Methods B 126(1–4):297–300
7. Richter S, Alonso A, De Bolle W, Wellum R, Taylor PDP (1999) Isotopic "fingerprints" for natural uranium ore samples. Int J Mass Spectrom 193(1):9–14
8. Berkovits D, Feldstein H, Ghelberg S, Hershkowitz A, Navon E, Paul M (2000) 236U in uranium minerals and standards. Nucl Instrum Methods B 172:372–376
9. Boulyga SF, Heumann KG (2006) Determination of extremely low ^{236}U/^{238}U isotope ratios in environmental samples by sector-field inductively coupled plasma mass spectrometry using high-efficiency sample introduction. J Environ Radioact 88(1):1–10
10. Ferguson JW, Houk RS (2006) High resolution studies of the origins of polyatomic ions in inductively coupled plasma-mass spectrometry, Part I. Identification methods and effects of neutral gas density assumptions, extraction voltage, and cone material. Spectrochim Acta B 61(8):905–915
11. Newman K, Freedman PA, Williams J, Belshaw NS, Halliday AN (2009) High sensitivity skimmers and non-linear mass dependent fractionation in ICP-MS. J Anal At Spectrom 24(6):742–751
12. Newman K (2012) Effects of the sampling interface in MC-ICP-MS: relative elemental sensitivities and non-linear mass dependent fractionation of Nd isotopes. J Anal At Spectrom 27(1):63–70
13. Oh SY, Lee SA, Park JH, Lee M, Song K (2012) Isotope measurement of uranium at ultratrace levels using multicollector inductively coupled plasma mass spectrometry. Mass Spectrom Lett 3(2):54–57
14. Mitroshkov AV, Olsen KB, Thomas ML (2015) Estimation of the formation rates of polyatomic species of heavy metals in plutonium analyses using a multicollector ICP-MS with a desolvating nebulizer. J Anal At Spectrom 30(2):487–493